JGR Biogeosciences

RESEARCH ARTICLE
10.1029/2020JG005823

Topographical Controls on Hillslope-Scale Hydrology Drive Shrub Distributions on the Seward Peninsula, Alaska

Zelalem A. Mekonnen[1], William J. Riley[1], Robert F. Grant[2], Verity G. Salmon[3], Colleen M. Iversen[3], Sébastien C. Biraud[1], Amy L. Breen[4], and Mark J. Lara[5,6]

[1]Climate and Ecosystem Sciences Division, Lawrence Berkeley National Laboratory, Berkeley, CA, USA, [2]Department of Renewable Resources, University of Alberta, Edmonton, AB, Canada, [3]Oak Ridge National Laboratory, Environmental Sciences Division and Climate Change Science Institute, Oak Ridge, TN, USA, [4]International Arctic Research Center, University of Alaska, Fairbanks, AK, USA, [5]Department of Plant Biology, University of Illinois, Urbana, IL, USA, [6]Department of Geography, University of Illinois, Urbana, IL, USA

Key Points:

- Topography and landscape hydrology are key environmental controls on observed Arctic shrub expansion of the past three decades
- Lateral flows of water, nutrients, and energy across slopes control nitrogen (N) mineralization, root O_2 and plant N uptakes, and thus plant composition
- N_2-fixing deciduous shrubs were shown to benefit more from a higher resource environment driven by enhanced mineralization

Supporting Information:

- Supporting Information S1
- Supporting Information S2

Correspondence to:

Z. A. Mekonnen,
zmekonnen@lbl.gov

Citation:

Mekonnen, Z. A., Riley, W. J., Grant, R. F., Salmon, V. G., Iversen, C. M., Biraud, S. C., et al. (2021). Topographical controls on hillslope-scale hydrology drive shrub distributions on the Seward Peninsula, Alaska. *Journal of Geophysical Research: Biogeosciences*, *126*, e2020JG005823. https://doi.org/10.1029/2020JG005823

Received 2 MAY 2020
Accepted 28 OCT 2020

Abstract Observations indicate shrubs are expanding across the Arctic tundra, mainly on hillslopes and primarily in response to climate warming. However, the impact topography exerts on hydrology, nutrient dynamics, and plant growth can make untangling the mechanisms behind shrub expansion difficult. We examined the role topography plays in determining shrub expansion by applying a coupled transect version of a mechanistic ecosystem model (*ecosys*) in a tundra hillslope site in the Seward Peninsula, Alaska. Modeled biomass of the dominant plant functional types agreed well with field measurements ($R^2 = 0.89$) and accurately represented shrub expansion over the past 30 years inferred from satellite observations. In the well-drained crest position, canopy water potential and plant nitrogen (N) uptake was modeled to be low from plant and microbial water stress. Intermediate soil water content in the mid-slope position enhanced mineralization and plant N uptake, increasing shrub biomass. The deciduous shrub growth in the mid-slope position was further enhanced by symbiotic N_2 fixation primed by increased root carbon allocation. The gentle slope in the poorly drained lower-slope position resulted in saturated soil conditions that reduced soil O_2 concentrations, leading to lower root O_2 uptake and lower nutrient uptake and plant biomass. A simulation that removed topographical interconnectivity between grid cells resulted in (1) a 28% underestimate of mean shrub biomass and (2) over or underestimated shrub productivity at the various hillslope positions. Our results indicate that land models need to account for hillslope-scale coupled surface and subsurface hydrology to accurately predict current plant distributions and future trajectories in Arctic ecosystems.

Plain Language Summary Several observations have shown that shrubs are expanding across the Arctic tundra. Most of these observations indicate that shrubs are expanding mainly on hillslopes and the processes through which topography controls shrub expansion remain unclear. We showed here, from our modeling analysis, that topographic controls on lateral surface and subsurface fluxes of water, nutrients, and energy affect the productivity and distributions of shrubs across the Kougarok watershed, Seward Peninsula, Alaska. Consistent with field measurements, the fast-growing deciduous shrubs were modeled to dominate the hillslope position with intermediate soil water content and higher nutrients. We conclude that surface and subsurface drainage hinders model performance in topographically diverse tundra landscapes.

1. Introduction

Numerous repeated-photography studies and plot-based long-term monitoring experiments show that shrubs are expanding across the Arctic tundra in response to warming (Chapin et al., 1995; Cornelissen et al., 2001; Elmendorf et al., 2012; Myers-Smith et al., 2011; Tremblay et al., 2012; Wahren et al., 2005; M. D. Walker et al., 2006). At regional scales, remote sensing observations indicate tundra topographical heterogeneity may influence the spatial variability and trajectory of shrub cover change (Berner et al., 2018; Frost et al., 2014; Lara et al., 2018). At the watershed scale, repeat oblique aerial photography confirms these observations, while identifying tundra hillslopes and terraces as hotspots of shrub expansion (Naito

& Cairns, 2011; Ropars & Boudreau, 2012; Tape et al., 2006), likely associated with higher resource environments (Tape et al., 2012). Although, research suggests topographic gradients may strongly influence shrub expansion (e.g., Frost et al., 2014; Swanson, 2015; Tape et al., 2012), the mechanisms through which topography controls shrub growth remains unclear (Martin et al., 2017).

Topographic gradients on tundra hillslopes influence many soil, vegetation, and hydrological factors that affect nutrient and carbon dynamics (Matthes-Sears et al., 1988; Moore et al., 1993). A number of tundra ecosystem studies reported strong relationships between moisture gradients and productivity (Bliss et al., 1984; Chapin et al., 1988; Engstrom et al., 2005; Lara et al., 2018; Matthes-Sears et al., 1988; Ostendorf & Reynolds, 1993). Hillslope hydrology is one of the major factors that affects northern ecosystem soil development (Moore et al., 1993), nutrients (Chu & Grogan, 2010; Rastetter et al., 2004), soil physical and chemical properties (Tromp-van Meerveld & McDonnell, 2006), shrub distribution (Matthes-Sears et al., 1988), and carbon cycling (Grant et al., 2015a; D. A. Walker, 2000). Furthermore, topography influences snow accumulation and spatial distribution (Essery & Pomeroy, 2004; Young et al., 1997), with implications for soil temperature (Liston, 1999), lateral surface water movement, soil water content, and snowmelt water influxes (Darboux & Huang, 2005). Shallower soil depths may reduce ecosystem productivity by reducing soil water storage, potentially hastening soil drying (Mekonnen et al., 2016).

Soil water content also affects soil-plant-atmosphere gas exchange and vertical diffusion. Saturated soil decreases gaseous diffusion into the soil by decreasing open pore space, limiting O_2 availability for plant uptake, and thereby reducing respiration and hence nutrient uptake by roots and microbes (Grable, 1966; Ponnamperuma, 1984). Soil water content is affected by the balance of precipitation and evapotranspiration and by surface and subsurface vertical and lateral water flows across hillslopes (Burt & Butcher, 1985; Kirkby, 1988). Overall, a complex set of interacting factors affect soil water content and nutrient availability, both of which affect vegetation productivity across topography. Therefore, understanding the complex surface and subsurface processes of Arctic tundra watershed hydrology on hillslopes is crucial to predicting regional shrub expansion.

Although substantial evidence suggests topographic controls on shrub distributions are important (Naito & Cairns, 2011; Ropars & Boudreau, 2012; Swanson, 2015; Tape et al., 2006), mechanistic analyses of these processes has not been performed. Here we applied a mechanistic ecosystem model, *ecosys*, to examine the distribution and expansion of shrubs across the recently established Kougarok Hillslope NGEE Arctic site in the Seward Peninsula, Alaska. The Kougarok watershed was shown to undergo shrub expansion over the past decades inferred from remote sensing data (Salmon et al., 2019). The *ecosys* model has a well-tested, fully coupled soil-plant-atmosphere hydraulic scheme that operates in a coupled hillslope transect mode. This model allows surface and subsurface fluxes of water, nutrients, and energy across the landscape and is therefore uniquely suited to exploring topographical controls on Arctic shrub growth and expansion.

Ecosys has been applied at many Arctic tundra sites to study carbon and nitrogen dynamics, vegetation structure, hydrology, and thermal dynamics (e.g., Chang et al., 2019; Grant et al., 2003, 2011; Grant et al., 2015, 2017a, 2017b; Mekonnen et al., 2018b). The modeled energy and carbon fluxes have been rigorously tested against data from eddy covariance flux towers across several high-latitude ecosystems, e.g., coastal (Grant et al., 2003) and mesic ($0.69 < R^2 < 0.78$) (Grant et al., 2011) Arctic tundra. Recently, the model was applied to study microtopography, temperature, and precipitation effects on active layer depth ($R^2 = 0.61$) (Grant et al., 2017b) and carbon dynamics ($0.7 < R^2 < 0.9$) (Grant et al., 2017a) in polygonal tundra at Utqiaġvik, Alaska, and CO_2 exchange as affected by hydrology in Arctic mixed tundra and in a fen ($R^2 = 0.7$–0.8) (Grant, 2015; Grant et al., 2015) at Daring Lake, Canada. Both of these studies used the multidimensional spatial capability of *ecosys* and the model accurately represented spatially resolved CO_2 exchanges. The model was also tested against large-scale vegetation remote sensing products such as MODIS GPP and AVHRR NDVI across northern ecosystems (Mekonnen et al., 2018a, 2018b, 2019).

We hypothesize that topography at Kougarok Hillslope site controls soil water content, available nutrients, and shrub productivity. For locations along this hillslope gradient, we therefore predict that:

(1) in crest positions: low soil water content from shallower soil depth and lateral water outflow result in slow root water and nutrient uptake, slow mineralization, leaf water stress, and thereby limitation of shrub growth

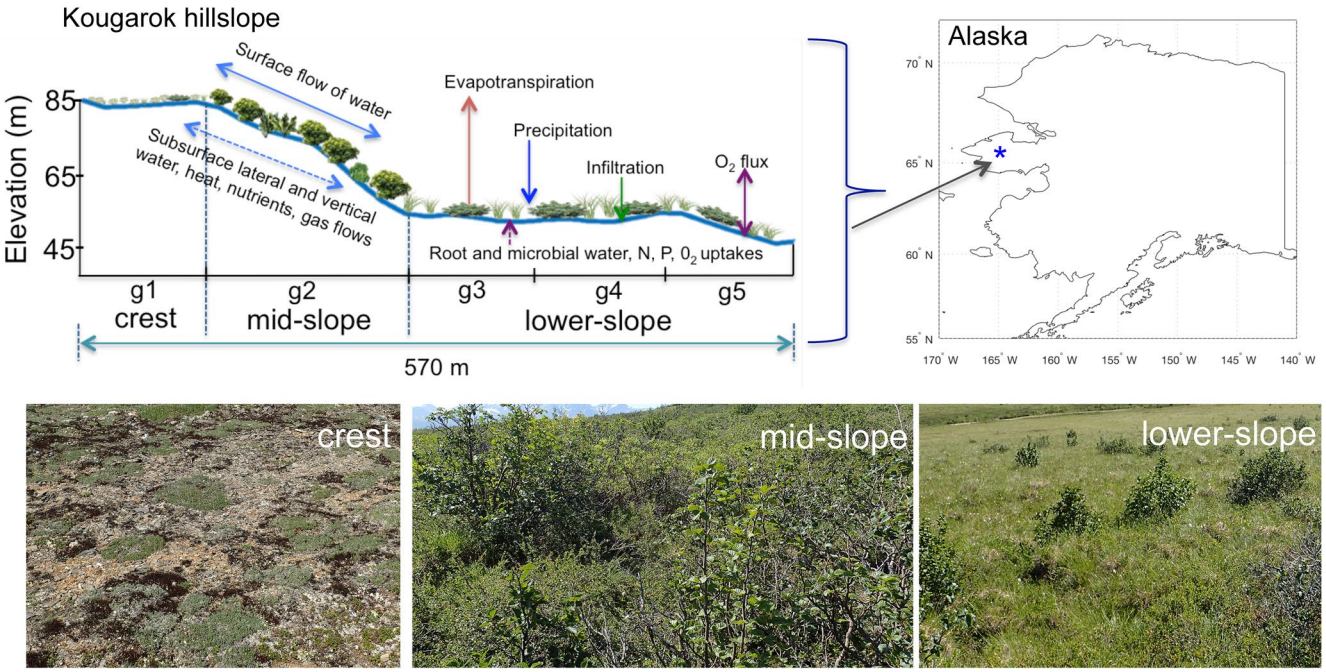

Figure 1. A schematic illustration of the major environmental controls on vegetation growth across Kougarok Hillslope positions as represented in the model. The coupled transect version of *ecosys* represents 2D topographic controls on surface and subsurface movement of water, heat, nutrients, and gasses. Five grid cells that represent three slope positions (Methods) were modeled across the Kougarok Hillslope transect (g1–g5, have dimensions of 85, 125, 120, 120, and 120 m, respectively). The slopes of each grid cells were derived from digital elevation model (Figure S1). Photos taken from Iversen et al. (2019).

(2) in mid-slope positions: intermediate soil water content from deeper soil and more rapid nutrient mineralization favors fast-growing plants (e.g., deciduous shrubs) associated with biological N_2 fixation; and
(3) in lower-slope positions: gentle slopes, deeper soils, and lateral water inflows result in saturated soil conditions, limiting O_2 availability, reducing root and microbial O_2 uptake, and thereby reducing active plant nutrient uptake and shrub growth

After benchmarking the model against observations from the Kougarok Hillslope (Salmon et al., 2017a, 2017b), we applied the model to characterize topographic controls on shrub distributions and expansion. The model allows coupling or decoupling of lateral interconnection of grid cells across topographic positions.

2. Materials and Methods

2.1. Site Description

The Kougarok Hillslope is located at 65° 09'43" N and 164° 48'39" W on the Kougarok watershed of Seward Peninsula, Alaska. The Kougarok watershed is covered by a variety of tundra vegetation including shrubs, graminoids, and nonvascular plants that vary in relative dominance and distribution across the hillslope position (Langford et al., 2019). The Kougarok Hillslope has distinct soil texture and moisture gradients: the crest of the hillslope has a shallow, drier rocky soil, the mid-slope position has well-drained soil dominated by alder shrubland, and the lower-slope position has wetter soil conditions (Salmon et al., 2019).

2.2. Simulation Design and Model Testing

2.2.1. Simulation Design

We modeled the productivity of shrubs in a transect along the east facing hillslope of the Kougarok watershed using *ecosys* (Figure 1; Figure S1). Five grid cells (g1–g5) along the transect were used to represent different slope positions (Figure 1). Grid cell slopes were determined from digital elevation model (Figure S1). *Ecosys* enables surface and subsurface lateral flows of water, nutrients, and energy over concentra-

tion gradients across interconnected grid cells. Grid cell positions are referred to as crest (g1, a nonacidic mountain complex with shallow soil depth, drier and coarser texture soil), mid-slope (g2, deeper soil, well-drained alder shrubland), and lower-slope (g3–g5, deeper soil with gentle slope, less drained tussock tundra; Figure 1). In all grid cells, the model was initialized with equal proportions of the five plant functional types (PFTs) present at this site: deciduous shrubs associated with biological N_2 fixation, evergreen shrubs, graminoids, and nonvascular plants (moss, lichen). The model was then run from 1950–2016. Climate forcing was obtained from the North American Regional Reanalysis (NARR) (Mesinger et al., 2006; Wei et al., 2014). The first 10 years of NARR (1979–1988) was cycled through 1950–1978 and the real time NARR was used from 1979–2016. Soil characteristics were obtained from 2016 field measurements (Salmon et al., 2017b) at the site (Table S1). To quantify the effects of topography on ecosystem productivity across the transect, we conducted a sensitivity simulation in the absence of topography (i.e., flat landscape without surface and subsurface lateral interconnection of grid cells) while keeping all other model inputs (i.e., soil properties, plant and microbial traits, and climate forcing) the same.

2.2.2. Model Testing

The modeled PFT and ecosystem aboveground biomass along the transect were quantitatively compared with 2016 biomass field measurements (Salmon et al., 2017a), and qualitatively compared with remote sensing observations of shrub cover. Modeled changes in shrub biomass were compared with estimated changes in shrub cover derived from high-resolution historical and contemporary multispectral image analysis (Figure S1b). The following procedure was used to derive estimates of shrub cover change: two cloud-free images (1) mid to late summer of 1985 (Alaska High Altitude Photography) and (2) 2014 (World View-2) were acquired from the Polar Geospatial Center, orthorectified, georeferenced (mean RMS error: 2.5 m), and resampled to 1 m resolution. We classified both multispectral images into dominant land cover classes (shrub, tussock, heath, rock, water, impervious) using a supervised support vector machine (SVM) algorithm. To avoid misclassifications associated with vegetation change, we used both 1985 and 2014 images to ensure reference data for SVM training was consistent across time (i.e., reference shrub patches were identifiable in both dates). The spatial distribution of the 2014 shrub classification was validated using a combination of ground-surveys and pan-sharpened World View-2 imagery (Salmon et al., 2019). Overall map accuracy was 91.9% ($n = 62$), achieving a Producer's accuracy of 94.7% and 90.6%, and the User's accuracy of 81.8% and 97.5% for shrub and nonshrub tundra, respectively. The geospatial shrub cover data was aggregated to the five slope positions across the Kougarok Hillslope transect within a 70-m buffer in 1985 and 2014, and compared with model outputs.

2.3. Model Description

As described in the Introduction section, the model has been successfully applied in several high-latitude ecosystems to study carbon, water, energy, and nutrient cycles and permafrost and vegetation dynamics. The mechanistic descriptions of the model processes most relevant to modeling surface and subsurface flows of water, heat, and gases across topography, effects of soil water content on CO_2 fixation, and nutrient dynamics are described below. A detailed model description, model algorithms, and parameters can be found in the supporting information S2 (S1: Soil C, N and P Transformations; S2: Soil-Plant Water Relations; S3: Gross Primary Productivity, Autotrophic Respiration, Growth and Litterfall; S4: Soil Water, Heat, Gas and Solute Fluxes; S5: Solute Transformations; S6: N_2 Fixation; S7: CH_4 Production and Consumption; S8: Inorganic N Transformations).

2.3.1. Surface and Subsurface Water Flows

Surface water flows across the hillslope transect are calculated from Manning's equation using runoff velocity, surface geometry, and slope (supporting information S2, S4). Runoff velocity is calculated from hydraulic radius, slope, and Manning's roughness coefficient. Changes in surface water depth are calculated from net surface flows of water and from precipitation versus evapotranspiration and infiltration among adjacent grid cells. Subsurface water fluxes are the product of hydraulic conductance and the differences in soil water potential of adjacent grid cells along the transect. The water potential of each grid cell is the sum of matric, osmotic, and gravitational potentials. Changes in soil water content are computed from differences in lateral subsurface flows among adjacent grid cells and from root water uptake within each grid cell. Subsurface

flows of water across adjacent grid cells are calculated from Richard's or Green-Ampt equations depending on the soil water potentials of the grid cells (Grant, 2004). Richard's equation is used if both source and destination grid cells are unsaturated, using unsaturated conductance and water potentials of the grid cells. The Green-Ampt equation is used if one of the grid cells is saturated, using saturated conductance and soil water potential beyond the wetting front of the unsaturated grid cell (Grant et al., 2004).

2.3.2. Heat and Gas Transfers

Conductive and convective heat transfers through the snowpack, surface litter, and soil layers are driven by surface heat fluxes calculated from closures of the energy balances at canopy, snowpack, surface litter, and soil surfaces (Grant et al., 1999). In a permafrost site, changes in soil ice content are used to calculate active layer depth, modeled from the general heat flux equation driven by surface energy exchange and subsurface heat transfer (Grant et al., 2019a). These heat fluxes drive freezing, thawing, and temperature dynamics in the snowpack, surface litter, and soil layers (Grant et al., 2015). Gaseous and aqueous concentration gradients drive volatilization and dissolution of gases between gaseous and aqueous phases of the soil and roots of each layer, and between the atmosphere and the aqueous phase at the soil surface of each grid cell. These gradients also drive soil convective and conductive gas transfers in gaseous and aqueous phases vertically within each grid cell, and laterally between adjacent grid cells using diffusivities calculated from air- and water-filled porosities. Gas transfers between the soil and the atmosphere through roots are driven by gaseous concentration gradients and diffusivities calculated from root porosities (Grant et al., 2017a). If the gaseous equivalent of the total partial pressure of all aqueous gases any soil layer exceeds atmospheric pressure, excess gas may be released by ebullition to the atmosphere.

2.3.3. Effects of Soil Water Content on CO_2 Fixation

Topography affects redistribution of snow in winter and surface water during snowmelt and summer precipitation events, thereby controlling soil water availability. The soil-plant-atmosphere water transfer scheme of the model simulates plant water status from a convergence solution for the canopy water potential at which canopy transpiration equilibrates with total water uptake from all rooted soil layers (Grant et al., 1999). Water uptake from soil layers to the canopy is determined by the potential difference between canopy and each soil layer across soil and root hydraulic resistances (Grant et al., 2007b). Stomatal conductance determined from canopy water potential controls the rate of canopy transpiration. Canopy water potential and canopy resistance determines CO_2 fixation from stomatal and nonstomatal effects of canopy water status, through a convergence solution for intercellular and canopy gaseous CO_2 concentration at which rates of diffusion and CO_2 fixation are equal (Grant and Flanagan, 2007). The soil-plant-atmosphere water transfer scheme of the model enables simulation of CO_2 fixation under variable soil water content driven by topography and soil characteristics.

2.3.4. C and N Transformations

Differences in soil water content across topography determine O_2 availability for plant and microbial uptake. Soil C and N transformations are driven by oxidation-reduction reactions as affected by soil water content and O_2 concentrations (supporting information S2, S1). Lower soil water potential results in water stress on microbial decomposition; these effects are calculated from increased microbial aqueous density and reduced microbial access to substrate at low soil water content. Decomposition rates of organic matter-microbe complexes (coarse woody litter, fine nonwoody litter, manure, particulate organic matter, and humus) represented in the model are determined by the active biomass of heterotrophic microbial populations and the substrate concentration (Grant et al., 2006). Decomposition rates are controlled by soil temperature through an Arrhenius function and by soil water content through its effect on aqueous microbial concentrations. Soil temperature and soil water content are calculated from surface energy and water exchanges coupled with soil heat and water transfers through atmosphere-canopy-snow-surface residue-soil profiles (Grant et al., 2012). Decomposition generates dissolved organic carbon that drives microbial growth through heterotrophic respiration. PFTs in each grid cell across the hillslope compete for common resources of water and nutrients according to root density and root length prognostically modeled from allocation of nonstructural products of CO_2 fixation (Grant, 2016; Grant et al., 2007a). The model algorithms and parameters most relevant to soil C, N, and P transformations can be found in supporting information S2 (S1).

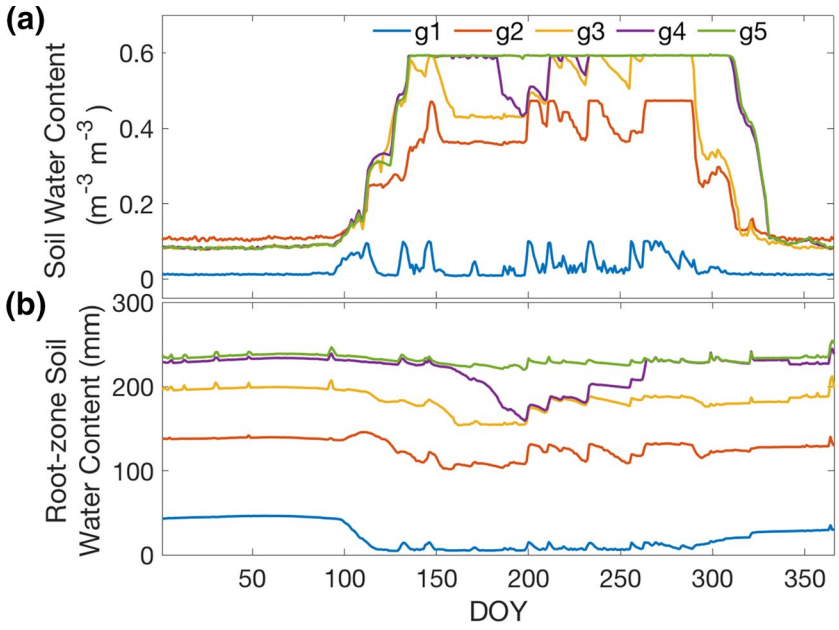

Figure 2. Modeled soil moisture was lowest in the crest position (g1), intermediate in the mid-slope position (g2), and highest in the lower-slope (g3, g4, g5) positions. Variations in modeled daily soil water content (a) at 5–10 cm depth and (b) integrated across the root-zone for the five laterally interconnected grid cells of the Kougarok Hillslope transect (g1-g5; Figure 1) in 2016.

Deciduous shrubs in the model support biological N_2 fixation thought symbiotic associations with bacteria (Grant et al., 2015). In the model, these plants meet part of their N requirements by exchanging fixed C from their roots or leaves for fixed N from the symbionts in root nodules that grow from nonstructural C, N, and P pools (C_n, N_n and P_n) exchanged with roots. During nodule growth, growth respiration, driven by autotrophic respiration of nodule C_n, drives uptake of additional nodule C_n for biomass growth. Nodule growth also requires uptake of N_n and P_n, although the ratio of N_n:C_n in the nodules is usually less than that required for microbial growth (Grant et al., 2015).

3. Results

3.1. Hydrology Across Kougarok Hillslope

Differences in topographic positions and soil depth caused variations in soil water content across the Kougarok Hillslope (Figure 2). Measured maximum soil depth was generally shallower in the crest relative to lower-slope positions. The crest position (g1) had ~1/3rd the soil rooting depth (~12 cm) of the lower-slope positions (g3–g5) (~38 cm) and thus 5–10 cm soil water content was modeled to be lower in the crest versus lower-slope positions (Figure 2a). Within *ecosys*, daily soil water content in the root zone also varied across the hillslope (Figure 2b). These variations were mainly attributed to differences in total water holding capacity and vertical and lateral flow of water and redistribution of snow driven by variations in slope.

Snowmelt during spring (~DOY 100) resulted in increased modeled soil water content across the Kougarok Hillslope (Figure 2a). However, the modeled soil water content in the crest position rapidly declined, caused by lesser snow accumulation and downward snow redistribution to the mid and lower-slope positions, resulting in lower root-zone soil water content during much of the growing season (Figure 2b). The mid-slope position was modeled to be wetter than the crest position because of both lateral surface and subsurface water flow from the adjacent crest grid cell as well as deeper soil that held more water and thereby maintained intermediate soil water content through much of the summer. Lateral surface and subsurface flow of water and the gentle slope of the lower-slope position created more saturated soil conditions through most of the growing season (Figure 2a). These hydrological interactions across the hillslope led to the progressively later

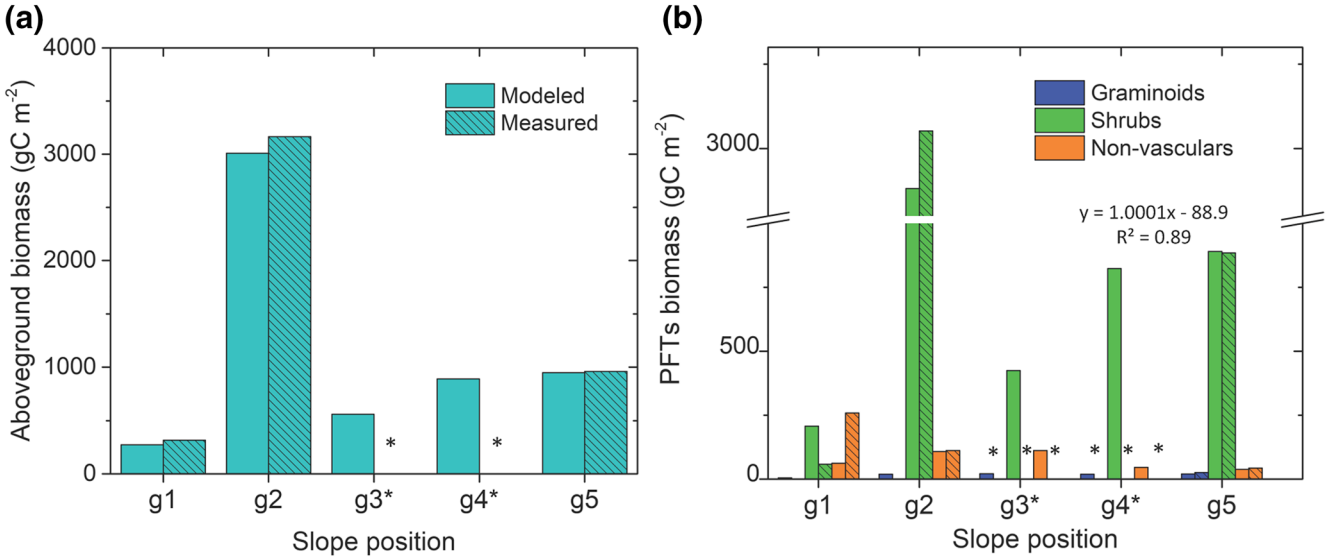

Figure 3. *Ecosys* accurately matched observations of (a) total ecosystem aboveground biomass and (b) plant functional types (PFTs) aboveground biomass ($R^2 = 0.89$; shrubs (deciduous + evergreen), graminoids, and nonvascular (moss + lichen)) across the Kougarok Hillslope transect in 2016. Hatched bars represent observations. * indicates missing biomass measurements for g3* and g4*.

initiation of root-zone soil water decreases from the crest (g1) down to the g4 lower-slope position, and for the more continuously saturated lower-slope position.

Modeled variation in soil water content across the hillslope was highest from DOY 150 through 280. The 5–10 cm soil in the crest position was much drier than the mid- and lower-slope positions throughout the summer (e.g., ~0.10, 0.45, and 0.60 $m^{-3}m^{-3}$, respectively during July; Figure 2a). Growing season soil water content remained intermediate in the mid-slope through DOY 270, despite a slight decline after snowmelt, which we partly attributed to higher summer transpiration rate of shrubs with larger aboveground biomass (Figure S2).

Spatial variation in transpiration rates across the transect were driven by differences in soil water content and ecosystem LAI (Figures S2 and S3d). Low transpiration limited by low soil water content and smaller LAI was modeled in the shallower crest position. The mid-slope position, with intermediate soil water content and high LAI, was modeled to have the greatest summer transpiration rates. Although the lower-slope position had the highest soil water content, its lower LAI (Figure S3d) resulted in lower transpiration compared to the mid-slope position.

3.2. Modeled Biomass Across the Kougarok Hillslope

Modeled ecosystem aboveground biomass agreed well with observed aboveground biomass in 2016 (Salmon et al., 2017a; Figure 3a). The model also accurately simulated the individual PFT's biomass ($R^2 = 0.89$) across the topographic gradient (Figure 3b). Total ecosystem productivity (Figure S3) and overall ecosystem aboveground biomass (Figure 3a), and shrub biomass in particular (Figure 3b), were modeled to vary across topographic positions. Observed and modeled shrubs had the largest aboveground biomass of all PFTs in the Kougarok Hillslope (Figure 3b).

We next used *ecosys* to explore the effects of topography on environmental conditions and processes relevant to shrub expansion, including water availability, N mineralization by soil microbes, biological N_2 fixation, CO_2 fixation, and plant growth. These conditions and processes interact with one another, potentially causing complex feedback loops. For example, the crest and lower-slope positions had significantly lower aboveground biomass than the mid-slope position (Figure 3a). In the well-drained and shallower soil depth crest position, lower soil water content reduced canopy water potential (Figure 4a) and thus stomatal conductance. Plant N uptake was low in the crest position (Figure 5) from lower water uptake and water stress

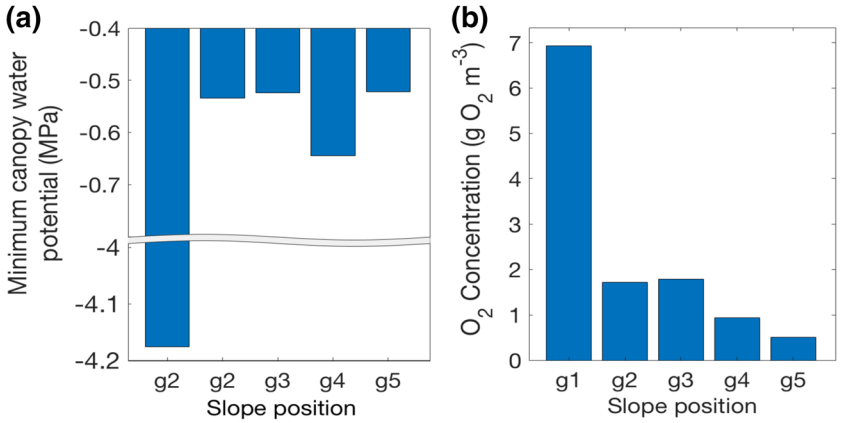

Figure 4. Modeled (a) minimum canopy water potential reached during each day (values between −1.5 and −2 MPa indicate mild water stress, values < −2 MPa indicate severe water stress) and (b) aqueous O_2 concentrations between 0 and 10 cm depth across the five grid cells (g1—g5) of the Kougarok Hillslope transect averaged for vascular plants during the peak growing season (July–August) in 2016.

on microbial decomposition and thus slower N mineralization, resulting in N limitation and thus lower CO_2 fixation and plant biomass (Figure 3a).

Intermediate soil water content in the mid-slope position did not strongly affect canopy water potential (Figure 4a). It also enhanced microbial mineralization and N_2 fixation that resulted in greater plant N uptake (Figure 5). This mid-slope position was also associated with high plant biomass (notably for N-fixing deciduous shrubs, Figure 3). High N availability with optimal soil water content increased modeled shrub growth, which resulted in shrubs dominating much of the mid-slope position (Figure 3b). The fast-growing deciduous versus evergreen shrubs dominated the mid-slope position from rapid N uptake that increased CO_2 fixation. The increase in the growth of deciduous shrubs was further increased by symbiotic N_2 fixation (Figure 5) primed by increased root carbon allocation. Shrub growth was also enhanced from greater

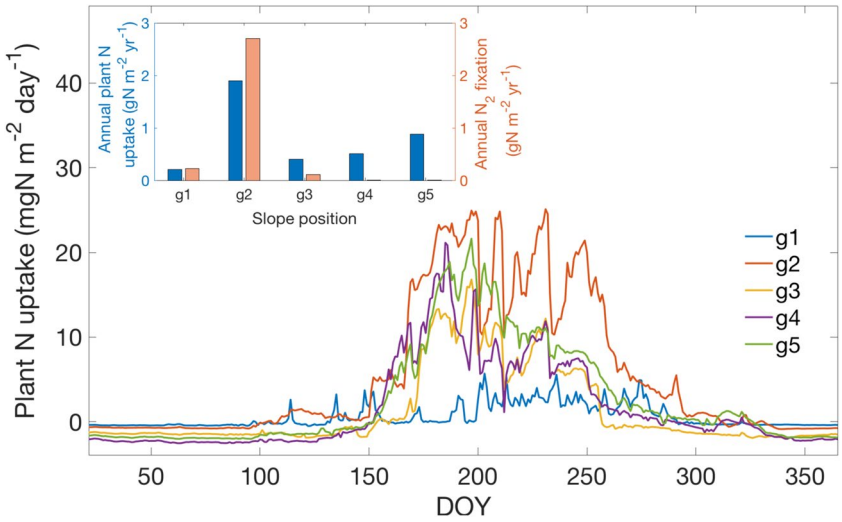

Figure 5. Modeled daily and annual plant nitrogen uptake and symbiotic N_2 fixation across the Kougarok Hillslope transect in 2016. Intermediate soil water content in the mid-slope position (g2; Figure 2) resulted in greater N-mineralization and thus plant nitrogen uptake. Besides the plant nitrogen uptake, the modeled symbiotic N_2 fixation in the root nodules of deciduous shrubs in the mid-slope position was modeled to be the highest across the transect. The deciduous shrubs were modeled to support biological N_2 fixation through symbiotic association with bacteria. The modeled N_2 fixation in the mid-slope position (2.7 gN m^{-2} yr^{-1}) is similar to field measurements (1.95 ± 0.68 gN m^{-2} yr^{-1}) obtained from adjacent plots (not located on our modeled transect) dominated by deciduous shrub (Alder shrubland) (Salmon et al., 2019).

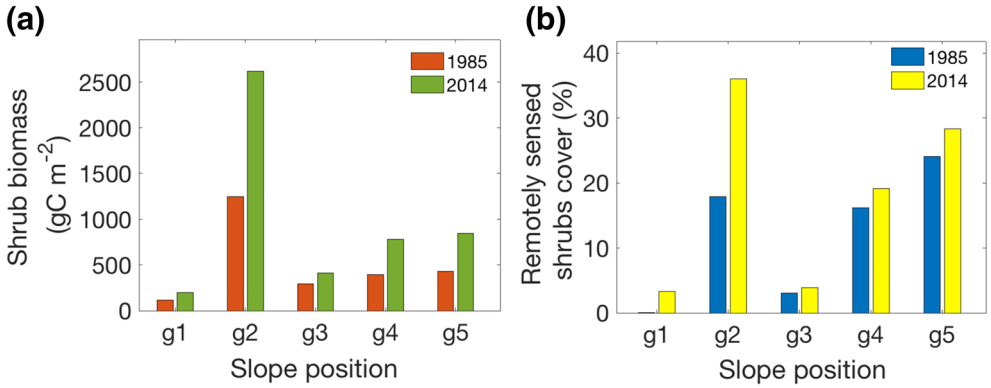

Figure 6. Satellite image-inferred cover changes and modeled shrub biomass changes were consistent, with the largest changes occurring in the mid-slope (g2) position. Changes in (a) modeled shrub biomass across the Kougarok Hillslope transect and (b) % of land covered by shrubs within the five slope positions across the Kougarok Hillslope that includes a 140 m buffer around the transect in 1985 versus 2014. Satellite image-inferred spatial average shrub area increased by ~48% from 1985 to 2014. Modeled shrub biomass across the hillslope transect increased by ~94% from 1985 from 2014. The modeled (transect) and satellite-derived metrics are not expected to be linearly related.

deciduous shrub litterfall and thereby increased mineralization from rapid decomposition of deciduous litter (smaller lignin fraction).

Lower biomass of shrubs was modeled in the lower-slope versus mid-slope position (Figure 3a). Saturated soil conditions (Figure 2) reduced soil O_2 concentrations (Figure 4b) and thus plant N uptake (Figure 5) in lower-slope positions. The reduced plant N uptake (Figure 5) under saturated soil conditions was modeled from lower microbial N mineralization and reduced plant root O_2 uptake by which active nutrient uptake was driven. Smaller growth of deciduous shrubs in the lower-slope position constrained symbiotic biological N_2 fixation (Figure 5) from limited root carbon availability.

3.3. Topography and Shrub Expansion

We tested whether observed increases in shrub cover between 1985 and 2014 on the Kougarok Hillslope were consistent with our model simulations. Modeled shrub biomass and NPP across the hillslope transect increased by ~94% (Figure 6) and ~20% (Figure S3), respectively, from 1985 to 2014, suggesting substantial potential for shrub expansion in recent decades. Using Kougarok Hillslope satellite images in 1985 and 2014, we estimate shrub cover increased ~48% over the 140 m-wide zone surrounding our model transect (Figure 6b). The largest proportional changes in both satellite image-inferred cover changes and modeled shrub biomass occurred in the mid-slope position, supporting our hypothesis that intermediate soil moisture positions are optimal for shrub growth. A direct comparison with the satellite image-inferred cover changes is not possible since *ecosys* does not predict "cover", but overall the observed shrub cover increases are consistent with modeled biomass and productivity increases over this 30-year period (Figure S3).

We next tested our hypothesis that lateral hydrological connectivity and thereby soil moisture variations are driving modeled and observed distributions of shrub biomass by simulating the same five grid cells without slope and interconnectivity between grid cells. Under this artificial model setup, which is common for many large-scale models (e.g., CLM (Lawrence et al., 2019); ELM (Zhu et al., 2019)), hillslope-scale shrub biomass was modeled to be much more homogeneous (Figure 7).

Ignoring topography caused over and underestimation of shrub productivity, depending on transect position (Figure 7). In the crest position (g1) the absence of grid cell interconnections led to a 68% increase in shrub aboveground biomass compared to simulations with interconnected grids (Table 1). Lack of surface and subsurface drainage to the downslope positions increased available soil water content in the shallower soil depth that subsequently enhanced vegetation productivity. Lack of drainage in the relatively deeper mid-slope (g2) resulted in a ~64% decline in shrub biomass while a slight increase of 13% was modeled across the lower-slope positions (averaged g3–g5) compared to the simulation with interconnected grids (Figure 7).

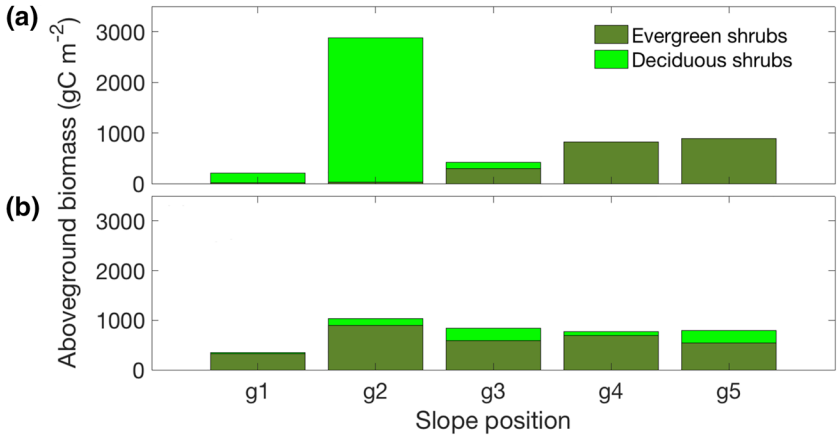

Figure 7. Modeled aboveground shrub biomass across the five Kougarok Hillslope transect grid cells for (a) the (default) coupled transect mode (which allowed lateral interconnection of grid cells) and (b) the artificial model geometry with a flat landscape without lateral interconnection of grid cells. Ignoring topography led to a 28% decrease in modeled shrub biomass across the transect and very different evergreen and deciduous shrub distributions.

Without the topography grid cell interconnectivity and the topography gradient, the relative biomass of evergreen and deciduous shrubs changed substantially. In this simulation, modeled high productivity of deciduous shrubs in the mid-slope position from intermediate soil water content could not be reproduced (Figure 7). The lack of grid cell interconnectivity also resulted in an increase in the relative fraction of mean biomass of evergreen shrubs (by 41%) with commensurate decline in the biomass fraction of deciduous shrubs. Overall, the mean shrub biomass across the transect was underestimated by 28% in the flat landscape versus interconnected grid cells across the true slope gradient.

4. Discussion

4.1. Topographic Controls on Vegetation Productivity

Modeled soil water content across topographic positions varied most during the peak growing season and least during shoulder seasons (Figure 2). Sustained moisture availability throughout summer was modeled to be a key factor that sustained plant water uptake and microbial decomposition. Modeled seasonality in soil water content is partly controlled by differences in transpiration rates across the hillslope (Figure S2). This conclusion is consistent with studies that showed spatial variation in vegetation distribution affecting

Table 1
Absolute and Percent Differences in Shrub Biomass in Coupled Transect Simulations With Interconnected Gridcells versus Flat Landscape Without Interconnected Gridcells in 2016 Across the Kougarok, AK Hillslope

	Difference in shrub biomass[a] (gCm^{-2})			Percent difference (%)[b]		
Slope position	Evergreen	Deciduous	Total	Evergreen	Deciduous	Total
g1	−168	308	140	−90	1464	67
g2	−2,706	860	−1846	−95	2655	−64
g3	131	285	416	104	96	98
g4	71	−124	−52	1362	−15	−6
g5	252	−352	−100	9819	−40	−11
Mean	−484	195	−289	−76	48	−28

[a]Difference in absolute evergreen, deciduous shrubs, and total (evergreen + deciduous) aboveground biomass (without interconnected grids–with interconnected grid cells) in 2016. [b]Percent difference in evergreen, deciduous shrubs, and total (evergreen + deciduous) aboveground biomass ((without interconnected grids–with interconnected grid cells)/interconnected grids biomass × 100) in 2016.

soil water content as a result of differences in evapotranspiration rates (Hupet & Vanclooster, 2002; Schume et al., 2003). The modeled lower soil water content in the crest position increases soil hydraulic resistance, which lowers canopy water potential (Figure 4a), stomatal conductance, and thus transpiration and CO_2 fixation rates. The mid-slope position, dominated by deciduous shrubs (Figure 3), had the highest transpiration rate (Figure 5) from faster water uptake resulting in higher nutrient uptake (and therefore CO_2 fixation).

Simulated soil water content was a key control on N mineralization, available N, and thus N uptake of co-existing PFTs across the hillslope. The mid-slope position had the highest N uptake (Figure 5), N_2 fixation, and transpiration, and thus fastest CO_2 fixation and largest deciduous shrub biomass (Figures 3 and 7). Our modeled differences in N availability driving tall shrub growth is consistent with other measurements that showed variations in microbial biomass, nutrient availability, tall shrub patches in hydrological diverse Arctic sites (Chu & Grogan, 2010; Matthes-Sears et al., 1988). The highest biological N_2 fixation was modeled in the mid-slope position (Figure 5) associated with greater net primary productivity and biomass (FiguresS3 andS7a). With greater supply of nonstructural C, deciduous shrubs meet part of their N requirements by exchanging fixed nonstructural C from their roots for fixed N from the symbionts in root nodules (Rhoades et al., 2001; Wallace & Baltzer, 2020) that grow from nonstructural C, N, and P pools exchanged with roots. With rapid shrub growth in the mid-slope position, nonwoody PFTs were not able to compete as a result of light interception of incoming direct and diffuse radiation by the tall shrubs.

The lower-slope positions had lower N availability and thus were dominated by evergreen versus deciduous shrubs, where the evergreen shrubs also had lower rates of N uptake. Relative dominance of deciduous versus evergreen shrubs in relation to differences in N uptake across the hillslope was modeled through differences in PFT specific functional traits that determine the strategy of resource acquisition and allocation (Bjorkman et al., 2018; Myers-Smith et al., 2019; Westoby et al., 2002; Wright et al., 2004) that drive growth, resource remobilization, and litterfall, and therefore plant species composition and abundance (Cahoon et al., 2012; Mekonnen et al., 2018b; Shaver et al., 2000).

A fast-growing strategy under greater N availability favored N_2-fixing deciduous shrub growth, which outcompeted evergreen shrubs, nonvascular plants, and graminoids in the mid-slope position (Figure 7a). However, the fast-growing deciduous shrubs were modeled to have less efficient nutrient conservation than evergreen shrubs, due to greater N loss from deciduous leaf turnover (Aerts, 1995; Mekonnen et al., 2018b). Rapid mineralization and plant N uptake (Figure 5) with intermediate soil water content in the mid-slope position further favored deciduous shrub growth (Figure 3b). Slower growing evergreen shrubs modeled with more efficient nutrient conservation (Aerts, 1995; Chapin and Shaver, 1989) dominated much of the lower slope with higher soil water content that created anaerobic conditions and inhibited N mineralization, thus limiting plant N uptake (Figure 7a). Root nutrient uptake requires root O_2 uptake to generate energy for active uptake processes (Grant et al., 2019b).

Modeled hydrological controls on N uptake and shrub growth on the Kougarok Hillslope highlight the importance of model representations of drainage conditions that influence soil nutrient dynamics. The simulated controls of nutrient availability on vegetation productivity along topographic gradients were consistent with studies linking hillslope drainage processes with the distribution of woody shrub biomass (Lloyd et al., 2003; Matthes-Sears et al., 1988; Rastetter et al., 2004; Tape et al., 2012) and vegetation composition (Miller, 1982; Murray & Miller, 1982; Rastetter et al., 2004). In an observational study at two Arctic tundra sites on the northern foothills of the Alaskan Brooks Range, Matthes-Sears et al. (1988) showed that high plant N and P concentrations measured in the drained part of the hillslope occurred because of higher soil nutrient availability. This result is consistent with our modeled variations in nutrient availability driven by topography and water drainage patterns that control plant N uptake and biomass across the slope (Figures 3 and 5).

4.2. Shrub Expansion and Topography

Our modeled increases in ecosystem productivity (Figure S3), LAI (Figure 6; Figure S3), and shrub expansion (Figure 6) over the last 3 decades are consistent with studies that have shown warming-enhanced

ecosystem productivity and shrub expansion across the Arctic tundra (Chapin et al., 1995; Cornelissen et al., 2001; Forbes et al., 2010). Besides warming, elevated atmospheric CO_2 enhances plant carbon uptake and biomass (Grulke et al., 1990). The satellite inferred and modeled increases in shrub productivity of the past decades (1985–2014) can be attributed to complex feedback mechanisms driven by climate, increases in atmospheric CO_2, and local hydrology as affected by topography. Using the Gradient Boosting Machine (GBM; Friedman, 2001) approach to test the nonlinear relationships and relative importance of these variables, we found that increases in atmospheric CO_2 and surface air temperature are the two most important distal factors in the relative long-term changes in modeled shrub biomass (Figure S4). However, since climate forcing and atmospheric CO_2 were the same for all grid cells, changes in the shrub biomass relative distribution across the hillslope were driven by local hydrology as affected by topography.

Further, the widely observed increases in Arctic tundra shrub cover have occurred preferentially on drained hillslopes rather than on saturated lowlands (Naito & Cairns, 2011; Ropars & Boudreau, 2012; Tape et al., 2006), consistent with our modeling results that illustrated important topographic controls on modeled shrub expansion across the Kougarok Hillslope in recent decades (Figure 6). Most of these previous observational studies reported changes in shrub cover, rather than biomass, which is more analogous, but not identical, to modeled changes in LAI. For example, a study by (Naito & Cairns, 2011), who used oblique aerial photographs in five areas in the northern slopes of Alaska from 1970–2000, reported −0.7%–46.6% increases in shrub cover on valley slopes. Tape et al. (2006) used 202 oblique aerial photographs in northern Alaska from 1999–2002 and reported 22%–30% increases in shrub cover, mostly on hillslopes and in valley bottoms. In a similar analysis of aerial photographs and satellite images from 1957–2008 in a subarctic site in Quebec, Canada, Ropars and Boudreau (2012) reported 11.6%–21.6% increases in shrub cover on hillslopes and terraces.

These observed shrub expansions have been shown to be related to hydrological characteristics driven by topographical differences. For instance, in five sites in Northern Alaska, Naito and Cairns (2011) concluded that drainage and soil water content were the major controls on shrub expansion across tundra hillslopes. Our modeled results also show that simulated shrub expansion is controlled by hillslope hydrology. In particular, the observed spatial heterogeneity of shrubs across the Kougarok Hillslope was not captured in our simulation that artificially ignored topography (Figure 7a), indicating that landscape hydrology is a crucial factor affecting shrub expansion. Although topographic controls of hillslope hydrology in watersheds have been represented in hydrological models (Bronstert, 1999; Clark et al., 2009; Ji et al., 2015; Stieglitz et al., 1999; Xiao et al., 1996), most large-scale land surface models use hydrologically disconnected grid cells (Hazenberg et al., 2016) and thus ignore landscape level heterogeneity in soil water content. These models are not able to capture landscape level heterogeneity in soil water content and nutrients, thus likely biasing their predictions of tundra shrub expansion. Our modeling results highlight interactions between hydrological controls as affected by topographic position and ongoing shrub expansion in response to recent climate change, and are consistent with observed expansion from long-term repeated photography (Tape et al., 2006; Tremblay et al., 2012) and warming experiments (Chapin et al., 1995; Cornelissen et al., 2001).

In addition to total shrub productivity, modeled heterogeneity in PFT productivity was shown to be controlled by topographic position (Figure 3b). *Ecosys* accurately captured the observed PFT biomass and their relative dominance (Figure 3b) across the Kougarok Hillslope transect, lending credibility to the model's ability to predict the trajectory of Arctic shrub cover under past and future climates. For instance, modeled intermediate soil water content favored shrub growth, consistent with measurements (Salmon et al., 2017a; Figure 3b). Similarly, Spadavecchia et al. (2008) reported that topographic variables explained most of the variations in plant distributions at an Arctic tundra site. The widely observed expansion of deciduous shrubs (e.g., alder) in recent decades in Arctic tundra (Fraser et al., 2014; Frost & Epstein, 2014; Frost et al., 2013) is an important response of the model, which was accurately captured as a result of simulating landscape hydrology in a coupled transect mode (Figure 7).

Overall, our simulation with no topographically driven drainage (i.e., an unrealistically flat and unconnected landscape; Figure 7b) substantially underestimated shrub growth. This finding is important because ∼36% of Circumpolar Arctic landscapes are classified as hills and mountains (Figure S5; based on topographical data from the CAVM-Team et al. (2003)). Therefore, underestimation of modeled shrub productivity in the

simulation with the artificially flat landscape has important implications for current model predications and model development of tundra ecosystem PFT dynamics and future ecosystem climate feedbacks.

5. Conclusions

We used a coupled transect version of the terrestrial ecosystem model *ecosys*, with interconnected grid cells that allow surface and subsurface fluxes of water, nutrients, and energy, to predict shrub productivity across the Kougarok Hillslope, Alaska. The model simulated aboveground biomass of PFTs across the transect that agreed well with measurements ($R^2 = 0.89$). Hillslope hydrology, and thus available soil water, was the major control on modeled soil microbial nutrient mineralization, availability of N for plant uptake, CO_2 fixation, and thus shrub productivity and expansion. Modeled fast-growing, N_2-fixing deciduous shrubs mostly dominated the hillslope position with intermediate soil water content and higher nutrient mineralization.

Our study corroborates hypothesized controls on shrub expansion posed by empirical studies (Martin et al., 2017; Tape et al., 2012) by mechanistically linking shrub distributions with higher resource environments affected by surface and subsurface water flow. We applied a model version with an artificially flat landscape to test this conclusion and found that ignoring topography led to: (1) underestimated mean shrub productivity by 28% and (2) poorly captured spatial heterogeneity in deciduous compared with evergreen shrubs. These results indicate that not representing surface and subsurface drainage hinders model performance in topographically diverse tundra landscapes. Earth system models that do not account for the underlying mechanisms of relatively fine-spatial scale surface and subsurface water, nutrients, and energy flows may therefore predict biased current and future distributions of Arctic PFTs.

Data Availability Statement

Data products in this study will be archived at http://ngee-arctic.ornl.gov.

Acknowledgments
This research was supported by the Director, Office of Science, Office of Biological and Environmental Research of the US Department of Energy under contract no. DE-AC02-05CH11231 to Lawrence Berkeley National Laboratory as part of the Next-Generation Ecosystem Experiments in the Arctic (NGEE-Arctic) project and the RUBISCO Scientific Focus Area of the RGMA program. We thank numerous people for the sample collection and processing needed to generate the empirical data used to inform this modeling analysis. Oak Ridge National Laboratory is managed by UT-Battelle, LLC for the United States Department of Energy under Contract Number DE-AC05-00OR22725. The United States Government retains and the publisher, by accepting the article for publication, acknowledges that the United States Government retains a nonexclusive, paid-up, irrevocable, world-wide license to publish or reproduce the published form of this manuscript, or allow others to do so, for United States Government purposes. The Department of Energy will provide public access to these results of federally sponsored research in accordance with the DOE Public Access Plan (http://energy.gov/downloads/doe-public-access-plan). We are grateful for the geospatial support provided by the Polar Geospatial Center under NSF PLR awards 1043681 and 1559691, and NSF Environmental Engineering award 1928048.

References

Aerts, R. (1995). The advantages of being evergreen. *Trends in Ecology & Evolution*, *10*(10), 402–407. https://doi.org/10.1016/s0169-5347(00)89156-9

Berner, L. T,, Jantz, P., Tape, K. D,., & Goetz, S. J. (2018). Tundra plant above-ground biomass and shrub dominance mapped across the North Slope of Alaska. *Environmental Research Letters*, *13*(3), 035002. http://dx.doi.org/10.1088/1748-9326/aaaa9a

Bjorkman, A. D., Myers-Smith, I. H., Elmendorf, S. C., Normand, S., Rüger, N., Beck, P. S., et al. (2018). Plant functional trait change across a warming tundra biome. *Nature*, *562*(7725), 57–62. http://dx.doi.org/10.1038/s41586-018-0563-7

Bliss, L., Svoboda, J., & Bliss, D. (1984). Polar deserts, their plant cover and plant production in the Canadian High Arctic. *Ecography*, *7*(3), 305–324. https://doi.org/10.1111/j.1600-0587.1984.tb01136.x

Bronstert, A. (1999). Capabilities and limitations of detailed hillslope hydrological modelling. *Hydrological Processes*, *13*(1), 21–48. https://doi.org/10.1002/(SICI)1099-1085(199901)13:1%3C21::AID-HYP702%3E3.0.CO;2-4

Burt, T., & Butcher, D. (1985). Topographic controls of soil moisture distributions. *Journal of Soil Science*, *36*(3), 469–486. https://doi.org/10.1111/j.1365-2389.1985.tb00351.x

Cahoon, S. M., Sullivan, P. F., Shaver, G. R., Welker, J. M., & Post, E. (2012). Interactions among shrub cover and the soil microclimate may determine future Arctic carbon budgets. *Ecology Letters*, *15*(12), 1415–1422. https://doi.org/10.1111/j.1461-0248.2012.01865.x

CAVM-Team, M., Walker, D. A., & Trahan, N. G. (2003). *Circumpolar Arctic vegetation. Scale 1:7,500,000*. US Fish and Wildlife Service. Retrieved from https://arcticatlas.org/maps/themes/cp/cpvg

Chang, K. Y., Riley, W. J., Crill, P. M., Grant, R. F., Rich, V. I., & Saleska, S. R. (2019). Large carbon cycle sensitivities to climate across a permafrost thaw gradient in subarctic Sweden. *The Cryosphere*, *13*(2), 647–663. http://dx.doi.org/10.5194/tc-13-647-2019

Chapin, F. S., Fetcher, N., Kielland, K., Everett, K. R., & Linkins, A. E. (1988). Productivity and nutrient cycling of Alaskan tundra: Enhancement by flowing soil water. *Ecology*, *69*(3), 693–702. https://doi.org/10.2307/1941017

Chapin, F. S., & Shaver, G. R. (1989). Differences in Growth and Nutrient use Among Arctic Plant Growth Forms. *Functional Ecology*, *3*(1), 73. http://dx.doi.org/10.2307/2389677

Chapin, F. S., Shaver, G. R., Giblin, A. E., Nadelhoffer, K. J., & Laundre, J. A. (1995). Responses of arctic tundra to experimental and observed changes in climate. *Ecology*, *76*(3), 694–711. https://doi.org/10.2307/1939337

Chu, H., & Grogan, P. (2010). Soil microbial biomass, nutrient availability and nitrogen mineralization potential among vegetation-types in a low arctic tundra landscape. *Plant and Soil*, *329*(1-2), 411–420. http://dx.doi.org/10.1007/s11104-009-0167-y

Clark, M. P., Rupp, D. E., Woods, R. A., Tromp-van Meerveld, H. J., Peters, N. E., & Freer, J. E. (2009). Consistency between hydrological models and field observations: Linking processes at the hillslope scale to hydrological responses at the watershed scale. *Hydrological Processes: An International Journal*, *23*(2), 311–319. http://dx.doi.org/10.1002/hyp.7154

Cornelissen, J. H., Callaghan, T. V., Alatalo, J., Michelsen, A., Graglia, E., Hartley, A., et al. (2001). Global change and arctic ecosystems: Is lichen decline a function of increases in vascular plant biomass?. *Journal of Ecology*, *89*(6), 984–994. https://doi.org/10.1111/j.1365-2745.2001.00625.x

Darboux, F., & Huang, C.-h. (2005). Does soil surface roughness increase or decrease water and particle transfers?. *Soil Science Society of America Journal*, *69*(3), 748–756. https://doi.org/10.2136/sssaj2003.0311

Elmendorf, S. C., Henry, G. H., Hollister, R. D., Björk, R. G., Bjorkman, A. D., Callaghan, T. V., et al. (2012). Global assessment of experimental climate warming on tundra vegetation: Heterogeneity over space and time. *Ecology Letters*, *15*(2), 164–175. https://doi.org/10.1111/j.1461-0248.2011.01716.x

Engstrom, R., Hope, A., Kwon, H., Stow, D., & Zamolodchikov, D. (2005). Spatial distribution of near surface soil moisture and its relationship to microtopography in the Alaskan Arctic coastal plain. *Hydrology Research*, *36*(3), 219–234. https://doi.org/10.2166/nh.2005.0016

Essery, R., & Pomeroy, J. (2004). Vegetation and topographic control of wind-blown snow distributions in distributed and aggregated simulations for an Arctic tundra basin. *Journal of Hydrometeorology*, *5*(5), 735–744. https://doi.org/10.1175/1525-7541(2004)005%3C0735:VATCOW%3E2.0.CO;2

Forbes, B. C., Fauria, M., & Zetterberg, P. (2010). Russian Arctic warming and 'greening'are closely tracked by tundra shrub willows. *Global Change Biology*, *16*(5), 1542–1554. https://doi.org/10.1111/j.1365-2486.2009.02047.x

Fraser, R. H., Lantz, T. C., Olthof, I., Kokelj, S. V., & Sims, R. A. (2014). Warming-induced shrub expansion and lichen decline in the Western Canadian Arctic. *Ecosystems*, *17*(7), 1151–1168. https://doi.org/10.1007/s10021-014-9783-3

Friedman, J. H. (2001). Greedy function Approximation: A gradient boosting machine. *Annals of Statistics*, 1189–1232.

Frost, G. V., & Epstein, H. E. (2014). Tall shrub and tree expansion in Siberian tundra ecotones since the 1960s. *Global Change Biology*, *20*(4), 1264–1277. https://doi.org/10.1111/gcb.12406

Frost, G. V., Epstein, H. E., & Walker, D. A. (2014). Regional and landscape-scale variability of Landsat-observed vegetation dynamics in northwest Siberian tundra. *Environmental Research Letters*, *9*(2), 025004. https://doi.org/10.1088/1748-9326/9/2/025004

Frost, G. V., Epstein, H. E., Walker, D. A., Matyshak, G., & Ermokhina, K. (2013). Patterned-ground facilitates shrub expansion in Low Arctic tundra. *Environmental Research Letters*, *8*(1), 015035. https://doi.org/10.1088/1748-9326/8/1/015035

Grable, A. R. (1966). Soil aeration and plant growth. *Advances in Agronomy*, *18*, 57–106. https://doi.org/10.1016/S0065-2113(08)60648-3

Grant, R. F. (2004). Modeling topographic effects on net ecosystem productivity of boreal black spruce forests. *Tree Physiology*, *24*(1), 1–18. https://doi.org/10.1093/treephys/24.1.1

Grant, R. F. (2015). Hydrological controls on ecosystem CO2 and CH4 exchange in a mixed tundra and a fen within an arctic landscape. Part 2. Modelled impacts of climate change. *Journal of Geophysical Research: Biogeosciences*, *120*, 13661387. https://doi.org/10.1002/2014JG002888

Grant, R. F. (2016). Ecological controls on N 2 O emission in surface litter and near-surface soil of a managed grassland: Modelling and measurements. *Biogeosciences*, *13*(12), 3549. https://doi.org/10.5194/bg-13-3549-2016

Grant, R. F., Baldocchi, D. D., & Ma, S. (2012). Ecological controls on net ecosystem productivity of a seasonally dry annual grassland under current and future climates: Modelling with ecosys. *Agricultural and Forest Meteorology*, *152*, 189–200. https://doi.org/10.1016/j.agrformet.2011.09.012

Grant, R. F., Black, T., Humphreys, E., & Morgenstern, K. (2007b). Changes in net ecosystem productivity with forest age following clearcutting of a coastal Douglas-fir forest: Testing a mathematical model with eddy covariance measurements along a forest chronosequence. *Tree Physiology*, *27*(1), 115–131. https://doi.org/10.1093/treephys/27.1.115

Grant, R. F., Wall, G., Kimball, B., Frumau, K., Pinter Jr, P., Hunsaker, D., & LaMorte, R., et al. (1999). Crop water relations under different CO_2 and irrigation: Testing of ecosys with the free air CO_2 enrichment (FACE) experiment. *Agricultural and Forest Meteorology*, *95*(1), 27–51. https://doi.org/10.1016/S0168-1923(99)00017-9

Grant, R. F., Black, T. A., Gaumont-Guay, D., Klujn, N., Barr, A. G., Morgenstern, K., & Nesic, Z., et al. (2006). Net ecosystem productivity of boreal aspen forests under drought and climate change: Mathematical modelling with Ecosys. *Agricultural and Forest Meteorology*, *140*(1–4), 152–170. https://doi.org/10.1016/j.agrformet.2006.01.012

Grant, R. F., Arkebauer, T. J., Dobermann, A., Hubbard, K. G., Schimelfenig, T. T., Suyker, A. E., et al. (2007a). Net Biome Productivity of Irrigated and Rainfed Maize–Soybean Rotations: Modeling vs. Measurements. *Agronomy Journal*, *99*(6), 1404. https://doi.org/10.2134/agronj2006.0308

Grant, R. F., Mekonnen, Z. A., Riley, W. J., Wainwright, H. M., Graham, D., & Torn, M. S. (2017). Mathematical Modelling of Arctic Polygonal Tundra with Ecosys : 1. Microtopography Determines How Active Layer Depths Respond to Changes in Temperature and Precipitation. *Journal of Geophysical Research: Biogeosciences*, *122*(12), 3161–3173. https://doi.org/10.1002/2017jg004035.

Grant, R. F., & Flanagan, L. B. (2007). Modeling stomatal and nonstomatal effects of water deficits on CO2 fixation in a semiarid grassland. *Journal of Geophysical Research*, *112*(G3), G03011. https://doi.org/10.1029/2006JG000302

Grant, R. F., Humphreys, E. R., & Lafleur, P. M. (2015). Ecosystem CO2 and CH4 exchange in a mixed tundra and a fen within a hydrologically diverse Arctic landscape: 1. Modeling versus measurements. *Journal of Geophysical Research: Biogeosciences*, *120*(7), 1366–1387. https://doi.org/10.1002/2014JG002888

Grant, R. F., Humphreys, E. R., Lafleur, P. M., & Dimitrov, D. D. (2011). Ecological controls on net ecosystem productivity of a mesic arctic tundra under current and future climates. *Journal of Geophysical Research: Biogeosciences*, *116*(G1), G01031. https://doi.org/10.1029/2010JG001555

Grant, R., Mekonnen, Z., & Riley, W. (2019a). Modeling climate change impacts on an Arctic polygonal tundra: 1. Rates of permafrost thaw depend on changes in vegetation and drainage. *Journal of Geophysical Research: Biogeosciences*, *124*(5), 1308–1322. https://doi.org/10.1029/2018JG004644

Grant, R. F., Mekonnen, Z. A., Riley, W. J., Arora, B., & Torn, M. S. (2017a). 2. Microtopography Determines How CO2 and CH4 Exchange Responds to Changes in Temperature and Precipitation at an Arctic Polygonal Tundra Site: Mathematical Modelling with Ecosys. *Journal of Geophysical Research: Biogeosciences*, *122*, 3174–3187. https://doi.org/10.1002/2017JG004037

Grant, R., Mekonnen, Z., Riley, W., Arora, B., & Torn, M. (2019b). Modelling climate change impacts on an Arctic polygonal tundra. Part 2: Changes in CO2 and CH4 exchange depend on rates of permafrost thaw as affected by changes in vegetation and drainage. *Journal of Geophysical Research: Biogeosciences*, *124*, 1323–1341. https://doi.org/10.1029/2018JG004645

Grant, R. F., Oechel, W. C., & Ping, C. L. (2003). Modelling carbon balances of coastal arctic tundra under changing climate. *Global Change Biology*, *9*(1), 16–36. https://doi.org/10.1046/j.1365-2486.2003.00549.x

Grulke, N., Riechers, G., Oechel, W., Hjelm, U., & Jaeger, C. (1990). Carbon balance in tussock tundra under ambient and elevated atmospheric CO 2. *Oecologia*, *83*(4), 485–494. https://doi.org/10.1007/BF00317199

Hazenberg, P., Broxton, P., Gochis, D., Niu, G. Y., Pangle, L., Pelletier, J. et al. (2016). Testing the hybrid-3-D hillslope hydrological model in a controlled environment. *Water Resources Research*, *52*(2), 1089–1107. https://doi.org/10.1002/2015WR018106

Hupet, F., & Vanclooster, M. (2002). Intraseasonal dynamics of soil moisture variability within a small agricultural maize cropped field. *Journal of Hydrology*, *261*(1), 86–101. https://doi.org/10.1016/S0022-1694(02)00016-1

Iversen, C., Breen, A., Salmon, V., VanderStel, H., & Wullschleger, S. (2019). NGEE Arctic plant traits: Vegetation plot locations, ecotypes, and photos, Kougarok road mile marker 64, Alaska, Seward Peninsula, 2016. *Next Generation Ecosystem Experiments Arctic Data Collection*, Oak Ridge, TN: Oak Ridge National Laboratory; U.S. Department of Energy. https://doi.org/10.5440/1346196

Ji, X., Shen, C., & Riley, W. J. (2015). Temporal evolution of soil moisture statistical fractal and controls by soil texture and regional groundwater flow. *Advances in Water Resources*, *86*, 155–169. https://doi.org/10.1016/j.advwatres.2015.09.027

Kirkby, M. (1988). Hillslope runoff processes and models. *Journal of Hydrology*, *100*(1–3), 315–339. https://doi.org/10.1016/0022-1694(88)90190-4

Langford, Z. L., Kumar, J., Hoffman, F. M., Breen, A. L., & Iversen, C. M. (2019). Arctic vegetation mapping using unsupervised training datasets and convolutional neural networks. *Remote Sensing*, *11*(1), 69. https://doi.org/10.3390/rs11010069

Lara, M. J., Nitze, I., Grosse, G., Martin, P., & McGuire, A. D. (2018). Reduced arctic tundra productivity linked with landform and climate change interactions. *Scientific Reports*, *8*(1), 2345. https://doi.org/10.1038/s41598-018-20692-8

Lara, M. J., Nitze, I., Grosse, G., & McGuire, A. D. (2018). Tundra landform and vegetation productivity trend maps for the Arctic Coastal Plain of northern Alaska. *Scientific Data*, 5(1). http://dx.doi.org/10.1038/sdata.2018.58.

Lawrence, D. M., Fisher, R. A., Koven, C. D., Oleson, K. W., Swenson, S. C., Bonan, G., et al. (2019). The Community Land Model version 5: Description of new features, benchmarking, and impact of forcing uncertainty. *Journal of Advances in Modeling Earth Systems*, *11*(12), 4245–4287. https://doi.org/10.1029/2018MS001583

Liston, G. E. (1999). Interrelationships among snow distribution, snowmelt, and snow cover depletion: Implications for atmospheric, hydrologic, and ecologic modeling. *Journal of Applied Meteorology*, *38*(10), 1474–1487. https://doi.org/10.1175/1520-0450(1999)038%3C1474:IASDSA%3E2.0.CO;2

Lloyd, A. H., Yoshikawa, K., Fastie, C. L., Hinzman, L., & Fraver, M. (2003). Effects of permafrost degradation on woody vegetation at arctic treeline on the Seward Peninsula, Alaska. *Permafrost and Periglacial Processes*, *14*(2), 93–101. https://doi.org/10.1002/ppp.446

Martin, A. C., Jeffers, E. S., Petrokofsky, G., Myers-Smith, I., & Macias-Fauria, M. (2017). Shrub growth and expansion in the Arctic tundra: An assessment of controlling factors using an evidence-based approach. *Environmental Research Letters*, *12*(8).085007. https://doi.org/10.1088/1748-9326/aa7989

Matthes-Sears, U., Matthes-Sears, W., Hastings, S., & Oechel, W. (1988). The effects of topography and nutrient status on the biomass, vegetative characteristics, and gas exchange of two deciduous shrubs on an arctic tundra slope. *Arctic and Alpine Research*, *20*, 342–351. https://doi.org/10.1080/00040851.1988.12002682

Mekonnen, Z. A., Grant, R. F., & Schwalm, C. (2016). Sensitivity of modeled NEP to climate forcing and soil at site and regional scales: Implications for upscaling ecosystem models. *Ecological Modelling*, *320*, 241–257. https://doi.org/10.1016/j.ecolmodel.2015.10.004

Mekonnen, Z. A., Riley, W. J., & Grant, R. F. (2018a). 21st century tundra shrubification could enhance net carbon uptake of North America Arctic tundra under an RCP8.5 climate trajectory. *Environmental Research Letters*, *13*(5).054029. https://doi.org/10.1088/1748-9326/aabf28

Mekonnen, Z. A., Riley, W. J., & Grant, R. F. (2018b). Accelerated nutrient cycling and increased light competition will lead to 21st century shrub expansion in North American Arctic tundra. *Journal of Geophysical Research: Biogeosciences*, *123*(5), 1683–1701. https://doi.org/10.1029/2017JG004319

Mekonnen, Z. A., Riley, W. J., Randerson, J. T., Grant, R. F., & Rogers, B. M. (2019). Expansion of high-latitude deciduous forests driven by interactions between climate warming and fire. *Nature Plants*, *5*, 952–958. https://doi.org/10.1038/s41477-019-0495-8

Mesinger, F., DiMego, G., Kalnay, E., Mitchell, K., Shafran, P. C., Ebisuzaki, W., et al. (2006). North American regional reanalysis. *Bulletin of the American Meteorological Society*, *87*(3), 343–360. https://doi.org/10.1175/BAMS-87-3-343

Miller, P. C. (1982). Environmental and vegetational variation across a snow accumulation area in montane tundra in central Alaska. *Ecography*, *5*(2), 85–98.

Moore, I. D., Gessler, P., Nielsen, G., & Peterson, G. (1993). Soil attribute prediction using terrain analysis. *Soil Science Society of America Journal*, *57*(2), 443–452.

Murray, C., & Miller, P. C. (1982). Phenological observations of major plant growth forms and species in montane and Eriophorum vaginatum tussock tundra in centralAlaska. *Ecography*, *5*(2), 109–116.

Myers-Smith, I. H., et al. (2011). Shrub expansion in tundra ecosystems: Dynamics, impacts and research priorities. *Environmental Research Letters*, *6*(4).045509.

Myers-Smith, I. H., Thomas, H. J., & Bjorkman, A. D. (2019). Plant traits inform predictions of tundra responses to global change. *New Phytologist*, *221*(4), 1742–1748. https://doi.org/10.1111/nph.15592

Naito, A. T., & Cairns, D. M. (2011). Relationships between Arctic shrub dynamics and topographically derived hydrologic characteristics. *Environmental Research Letters*, *6*(4).045506. https://doi.org/10.1088/1748-9326/6/4/045506

Ostendorf, B., & Reynolds, J. F. (1993). Relationships between a terrain-based hydrologic model and patch-scale vegetation patterns in an arctic tundra landscape. *Landscape Ecology*, *8*(4), 229–237. https://doi.org/10.1007/BF00125130

Ponnamperuma, F. (1984). CHAPTER 2 - Effects of flooding on soils. Kozlowskipp, T. T. (Ed.). In *Flooding and plant growth* (pp. 9–45). San Diego: Academic Press. https://doi.org/10.1016/B978-0-12-424120-6.50007-9

Rastetter, E. B., Kwiatkowski, B. L., Le Dizès, S., & Hobbie, J. E. (2004). The role of down-slope water and nutrient fluxes in the response of Arctic hill slopes to climate change. *Biogeochemistry*, *69*(1), 37–62. https://doi.org/10.1023/B:BIOG.0000031035.52498.21

Rhoades, C., Oskarsson, H., Binkley, D., & Stottlemyer, B. (2001). Alder (Alnus crispa) effects on soils in ecosystems of the Agashashok River valley, northwest Alaska. *Écoscience*, *8*(1), 89–95. https://doi.org/10.1080/11956860.2001.11682634

Ropars, P., & Boudreau, S. (2012). Shrub expansion at the forest–tundra ecotone: spatial heterogeneity linked to local topography. *Environmental Research Letters*, *7*(1).015501. https://doi.org/10.1088/1748-9326/7/1/015501

Salmon, V. G., Breen, A. L., Kumar, J., Lara, M. J., Thornton, P. E., Wullschleger, S. D., & Iversen, C. M., et al. (2019). Alder distribution and expansion across a tundra hillslope: Implications for local N cycling. *Frontiers of Plant Science*, *10*, 1099. https://doi.org/10.3389/fpls.2019.01099

Salmon, V., Iversen, C. & Breen, A., (2017a). *NGEE Arctic plant traits: Plant biomass and traits, Kougarok road mile marker 64, Seward Peninsula, Alaska, beginning 2016, next generation ecosystem experiments Arctic data collection*. Oak Ridge, TN, USA: Oak Ridge National Laboratory, U.S. Department of Energy. Dataset accessed on [02/28/2017] at https://doi.org/10.5440/1346199

Salmon, V. G., Iversen, C., Joanne, C. & Stel, H. V., (2017b). *NGEE Arctic plant traits: Soil cores, Kougarok road mile marker 64, Seward Peninsula, Alaska, 2016, next generation ecosystem experiments Arctic data collection*. Oak Ridge, TN, USA: Oak Ridge National Laboratory, U.S. Department of Energy. Dataset accessed on [02/28/2017] at https://doi.org/10.5440/1346200

Schume, H., Jost, G., & Katzensteiner, K. (2003). Spatio-temporal analysis of the soil water content in a mixed Norway spruce (Picea abies (L.) Karst.)–European beech (Fagus sylvatica L.) stand. *Geoderma*, *112*(3), 273–287. https://doi.org/10.1016/S0016-7061(02)00311-7

Shaver, G. R., Canadell, J., Chapin, F. S., Gurevitch, J., Harte, J., Henry, G., et al. (2000). Global warming and terrestrial ecosystems: A conceptual framework for analysis. *BioScience*, *50*(10), 871–882. https://doi.org/10.1641/0006-3568(2000)050[0871:GWATEA]2.0.CO;2

Spadavecchia, L., Williams, M., Bell, R., Stoy, P. C., Huntley, B., & Van Wijk, M. T., et al. (2008). Topographic controls on the leaf area index and plant functional type of a tundra ecosystem. *Journal of Ecology*, *96*(6), 1238–1251. https://doi.org/10.1111/j.1365-2745.2008.01424.x

Stieglitz, M., Hobbie, J., Giblin, A., & Kling, G. (1999). Hydrologic modeling of an arctic tundra watershed: Toward Pan-Arctic predictions. *Journal of Geophysical Research*, *104*(D22), 27507–27518. https://doi.org/10.1029/1999JD900845

Swanson, D. K. (2015). Environmental limits of tall shrubs in Alaska's Arctic National Parks. *PloS One*, *10*(9).e0138387. https://doi.org/10.1371/journal.pone.0138387

Tape, K. D., Hallinger, M., Welker, J. M., & Ruess, R. W. (2012). Landscape heterogeneity of shrub expansion in Arctic Alaska. *Ecosystems*, *15*(5), 711–724. https://doi.org/10.1007/s10021-012-9540-4

Tape, K., Sturm, M., & Racine, C. (2006). The evidence for shrub expansion in northern Alaska and the Pan-Arctic. *Global Change Biology*, *12*(4), 686–702. https://doi.org/10.1111/j.1365-2486.2006.01128.x

Tremblay, B., Lévesque, E., & Boudreau, S. (2012). Recent expansion of erect shrubs in the Low Arctic: Evidence from Eastern Nunavik. *Environmental Research Letters*, *7*(3),.035501. https://doi.org/10.1088/1748-9326/7/3/035501

Tromp-van Meerveld, H., & McDonnell, J. (2006). On the interrelations between topography, soil depth, soil moisture, transpiration rates and species distribution at the hillslope scale. *Advances in Water Resources*, *29*(2), 293–310. https://doi.org/10.1016/j.advwatres.2005.02.016

Wahren, C. H., Walker, M., & Bret-Harte, M. (2005). Vegetation responses in Alaskan arctic tundra after 8 years of a summer warming and winter snow manipulation experiment. *Global Change Biology*, *11*(4), 537–552. https://doi.org/10.1111/J.1365-2486.2005.00927.X

Walker, D. A. (2000). Hierarchical subdivision of Arctic tundra based on vegetation response to climate, parent material and topography. *Global Change Biology*, *6*(S1), 19–34. https://doi.org/10.1046/j.1365-2486.2000.06010.x

Walker, M. D., Wahren, C. H., Hollister, R. D., Henry, G. H., Ahlquist, L. E., Alatalo, J. M., et al. (2006). Plant community responses to experimental warming across the tundra biome. *Proceedings of the National Academy of Sciences*, *103*(5), 1342–1346. https://doi.org/10.1073/pnas.0503198103

Wallace, C. A., & Baltzer, J. L. (2020). Tall shrubs mediate abiotic conditions and plant communities at the taiga–tundra ecotone. *Ecosystems*, *23*(4), 828–841. https://doi.org/10.1007/s10021-019-00435-0

Wei, Y., Liu, S., Huntzinger, D., Michalak, A., Viovy, N., & Post, W., et al. (2014). NACP MsTMIP: Global and North American Driver Data for Multi-Model Intercomparison. *Data set*. Oak Ridge, TN: Oak Ridge National Laboratory Distributed Active Archive Center. https://doi.org/10.3334/ORNLDAAC/1220

Westoby, M., Falster, D. S., Moles, A. T., Vesk, P. A., & Wright, I. J. (2002). Plant ecological strategies: Some leading dimensions of variation between species. *Annual Review of Ecology and Systematics*, 125–159. https://doi.org/10.1146/annurev.ecolsys.33.010802.150452

Wright, I. J., Reich, P. B., Westoby, M., Ackerly, D. D., Baruch, Z., Bongers, F., et al. (2004). The worldwide leaf economics spectrum. *Nature*, *428*(6985), 821–827. https://doi.org/10.1038/nature02403

Xiao, Q. F., Ustin, S. L., & Wallender, W. W. (1996). A spatial and temporal continuous surface-subsurface hydrologic model. *Journal of Geophysical Research: Atmospheres*, *101*(D23), 29565–29584. https://doi.org/10.1029/96JD02210

Young, K. L., Woo, M.-k., & Edlund, S. A. (1997). Influence of local topography, soils, and vegetation on microclimate and hydrology at a high Arctic site, Ellesmere Island, Canada. *Arctic and Alpine Research*, 270–284. https://doi.org/10.1080/00040851.1997.12003245

Zhu, Q., et al. (2019). Representing nitrogen, phosphorus, and carbon interactions in the E3SM Land Model: Development and global benchmarking. *Journal of Advances in Modeling Earth Systems*, *11*, 2238–2258. https://doi.org/10.1029/2018MS001571